Core-Shell Structured PEO-Chitosan Nanofibers by Coaxial Electrospinning

ARTICLE *in* BIOMACROMOLECULES · FEBRUARY 2012

Impact Factor: 5.75 · DOI: 10.1021/bm201444v · Source: PubMed

3 AUTHORS, INCLUDING:

Mehdi Pakravan
Polytechnique Montréal
5 PUBLICATIONS **99** CITATIONS

Article

pubs.acs.org/Biomac

Core–Shell Structured PEO-Chitosan Nanofibers by Coaxial Electrospinning

Mehdi Pakravan, Marie-Claude Heuzey,* and Abdellah Ajji*

CREPEC, Department of Chemical Engineering, Ecole Polytechnique de Montreal, P.O. Box 6079, Station Centre-Ville, Montreal, Quebec, Canada H3C 3A7

Supporting Information

ABSTRACT: Core–shell structured PEO-chitosan nanofibers have been produced using a coaxial electrospinning setup. PEO and chitosan solutions, both in an aqueous acetic acid solvent, were used as the inner (core) and outer (shell) layer, respectively. Uniform-sized defect-free nanofibers of 150–190 nm diameter were produced. In addition, hollow nanofibers could be obtained subsequent to PEO washing of the membranes. The core–shell nanostructure and existence of chitosan on the shell layer were confirmed by TEM images obtained before and after washing the PEO content with water. The presence of chitosan on the surface of the composite nanofibers was further supported by XPS studies. The chitosan and PEO compositions in the nanofibrous mats were determined by TGA analysis, which were similar to their ratio in the feed solutions. The local compositional homogeneity of the membranes and the efficiency of the washing step to remove PEO were also verified by FTIR. In addition, DSC and XRD were used to characterize the crystalline structure and morphology of the co-electrospun nonwoven mats. The prepared coaxial nanofibers (hollow and solid) have several potential applications due to the presence of chitosan on their outer surfaces.

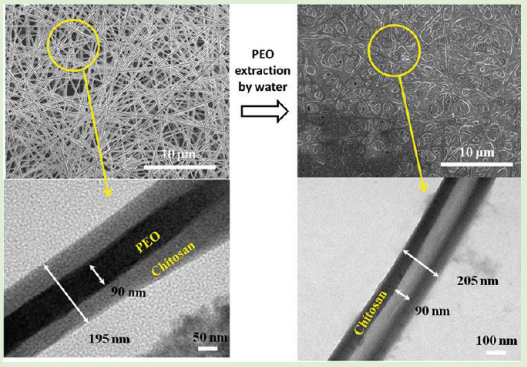

INTRODUCTION

There has been a growing interest for the fabrication of chitosan nanofibers in recent years due to a wide variety of potential applications such as antibacterial films,[1] membranes for metal ions removal,[2,3] supports for enzyme immobilization,[4] drug delivery systems,[5] tissue engineering scaffolds,[6,7] and wound healing dressings.[8] Electrospinning is a simple and continuous process that is used to generate submicrometer fibers in the form of nonwoven mats. In this process a charged polymer solution flows out of a syringe/needle setup and accelerates toward a collector, positioned at a fixed distance from the needle. Through electrostatic forces, a driven jet of polymer solution forms, elongates, and whips until it is deposited on the collector, resulting in the formation of nonwoven random nanofibers.[9] The resulting electrospun membranes exhibit remarkable characteristics such as distinctly high specific surface area (typically 20–100 m^2/g), high porosity, and small pore size.[10]

Chitosan is a modified natural polymer derived from chitin, one of the most abundant organic materials in the world. It is very similar to cellulose, except for the amino group replacing the hydroxyl group on the C-2 position. The $-NH_2$ groups on the chitosan backbone provide several unique properties such as solubility in acidic aqueous solvents, antifungal and antimicrobial properties, and the ability to chelate heavy metal ions.[11] The electrospinnability of chitosan is limited mostly by its polycationic nature in solution, rigid chemical structure, and specific inter- and intramolecular interactions.[12−14] The repulsive forces, arising from the protonation of the $-NH_2$ groups, may also restrict the formation of sufficient chain entanglements to allow successful electrospinning.[15,16]

Neat electrospun chitosan nanofibers have been prepared by dissolving chitosan in trifluoroacetic acid (TFA)[17] and its mixtures with dichloromethane (DCM) and trichloromethane (TCM).[18] TFA forms stable salts with the amino groups of chitosan, which can efficiently hinder the intermolecular interactions between chitosan chains and facilitate electrospinning.[17] A highly concentrated aqueous acetic acid solution (80–90%) was also reported by some research groups as another successful solvent for the fabrication of neat chitosan nanofibers, using chitosan grades with degrees of deacetylation (DDA) of 54[19] and 75–85%.[20] It is believed that decreasing the surface tension of the solution by increasing the acetic acid content can help the electrospinnability of chitosan.[19]

Applications of electrospun chitosan nanofibers using TFA-based solvents are however limited, as the prepared membranes can easily dissolve in neutral and weak basic aqueous solvents[21] due to the high solubility of the TFA-chitosan salt residues. Additionally, working with toxic and harmful solvents and the possible presence of their residues in the final membranes always raise major concerns.

Received: October 14, 2011
Revised: January 9, 2012
Published: January 9, 2012

Blending chitosan with materials that facilitate its processing is another approach to make chitosan electrospinnable. The co-spinning agent should have excellent fiber forming characteristics in order to create entanglements and physical bonds with chitosan, and act as a carrier in the electrospinning process. Synthetic polymers such as polyethylene oxide (PEO),[12,22−24] polyvinyl alcohol (PVA),[8,14] polylactic acid (PLA),[25] nylon-6,[26] polycaprolactone (PCL),[27] and proteins such as silk fibroin,[28] zein,[29] and collagen[30] have been successfully blended with chitosan to produce chitosan-based composite nanofibers. Generally, the content of the co-spinning agent varies from 20 to 80 wt %. The presence of this second phase can, however, affect the properties of the nanofibers by decreasing the chitosan content located at the surface. This influences properties such as biocompatibility and mechanical integrity and may be hard to rectify by an extraction process.

The coaxial electrospinning method provides an alternative and effective way of fabricating chitosan-based nanofibers. In this technique, two different solutions are spun simultaneously through a spinneret composed of two coaxial capillaries to produce core−shell structured nanofibers. Sun et al.[31] and Jian et al.[32] employed coaxial electrospinning to prepare nanofibers from polymer solutions with limited electrospinnability. They co-electrospun these solutions as the core material, with a readily electrospinnable solution as the shell layer to make core−shell nanofibers of the two components. Previously, Ojha et al.[33] used this method to prepare chitosan nanofibers by coaxial electrospinning of PEO as a template sheath for the chitosan core and then removal of the shell phase by water washing of PEO to expose the chitosan nanofibers.

In this paper we demonstrate that chitosan-based nanofibers with chitosan entirely located at the outer surface can be produced by a one-step coaxial electrospinning process, instead of the two-step method reported above. To the best of our knowledge, it is the first time that core−shell structured PEO-chitosan nanofibers are produced by a one-step coaxial electrospinning process, with chitosan as the shell component (outer layer) and PEO as the core material (inner layer) from aqueous solutions. Therefore, any post-treatment required to extract the PEO phase in order to have chitosan on the outer surface is eliminated. The produced nanofibers can have significant potential applications in the biomedical field involving wound care and tissue engineering due to the biocompatibility of both chitosan and PEO. Moreover, hollow chitosan nanofibers can be obtained by PEO washing of these coaxial nanofibers, which could also be of great interest in applications such as blood purification in hemodialysis.[34] In this work, the morphology and core/shell structure of produced nanofibers are studied by scanning electron microscopy (SEM) and transmission electron microscopy (TEM). The presence of chitosan on the outer layer is also confirmed by X-ray photoelectron spectroscopy (XPS) measurements. Bulk and local compositional analysis is performed by thermal gravimetry (TGA) and Fourier transform infrared spectroscopy (FTIR) techniques. Finally, differential scanning calorimetry (DSC) and X-ray diffraction (XRD) methods are utilized to investigate the crystalline structure of the prepared nanofibrous membranes.

EXPERIMENTAL SECTION

Materials. A commercial chitosan grade in the form of fine powder was supplied by Marinard Biotech (Rivière-au-Renard, QC, Canada). The weight-average molecular weight of this chitosan was measured by size exclusion chromatography with multiangle laser light scattering (SEC-MALLS) and was found to be 85 ± 5 kDa. The degree of deacetylation (DDA; 97.5%) was determined from ^{1}H NMR spectroscopy. More on the characterization of this chitosan grade can be found in ref 24. PEO, with a molecular weight of 600 kDa, was obtained from Scientific Polymers Inc. (Ontario, NY, U.S.A.). Reagent grade acetic acid (99.7%, Aldrich, WI, U.S.A.) was employed to prepare the aqueous solutions. All the materials were used as received.

Master Solutions. The chitosan solution was prepared at a concentration of 4 wt % in 50 wt % aqueous acetic acid. PEO solutions at 2, 3, and 4 wt % of polymer content were prepared in 50 wt % aqueous acetic acid and at 4 wt % in water. Solution mixing was performed at room temperature using a laboratory magnetic stirrer (Corning Inc., MA, U.S.A.) for 18−24 h to ensure complete dissolution of the polymers and obtain homogeneous solutions. The prepared solutions were left to rest 4 h for degassing and kept in sealed containers at room temperature.

Electrospinning. Coaxial electrospinning was performed using a horizontal setup containing a variable high DC voltage power supply (Gamma High Voltage Research, FL, U.S.A.) and a programmable microsyringe pump (Harvard Apparatus, PHD 2000, U.S.A.). Chitosan and PEO solutions were poured into 10 mL plastic syringes mounted on the pump with a multirack grip; hence, the flow rates of the core (PEO solution) and shell (chitosan solution) components were identical during the tests. The syringes were connected by plastic tubes and Luer-Lock connections to the inlets of a coaxial spinneret (Linari Engineering, Pisa, Italy). The coaxial spinneret was comprised of a 21-gauge (i.d. 0.510 mm, o.d. 0.830 mm) inner needle concentrically mounted on a 15-gauge (i.d. 1.37 mm, o.d. 1.83 mm) outer needle and was grounded by use of an alligator clip. The schematic outline of the coaxial electrospinning set up is shown in Figure 1. Blended chitosan/

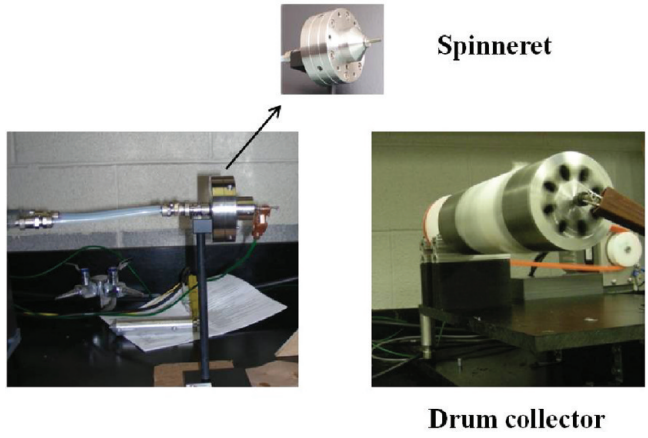

Figure 1. Schematic representation of the coaxial electrospinning setup.

PEO nanofibers were also produced for comparison purposes. Two chitosan/PEO blend solutions were prepared by mixing the two master solutions at 50/50 and 80/20 chitosan/PEO ratios. The blended solutions were poured into an 8 mL stainless steel syringe (Harvard Apparatus, U.S.A.) with a Luer-Lock connection to a 20-gauge blunt tip needle (Cadence Science, NY, U.S.A.). The syringe was mounted on the same electrospinning setup as for the coaxial electrospinning. More details on this procedure have been presented elsewhere.[24] Fiber mats were collected on an aluminum foil attached to a drum collector that could easily be removed for subsequent characterization. A homemade designed drum with both rotational and translational controllable movements was connected to the power supply 15 cm away from the needle. Samples were collected in both static and rotating drum mode, based on the requirements of the subsequent characterization techniques. Flow rates of 0.25−0.5 mL/h (in each syringe) and a voltage range of 15−20 kV were used as process parameters. The electrospinning parameters used were chosen

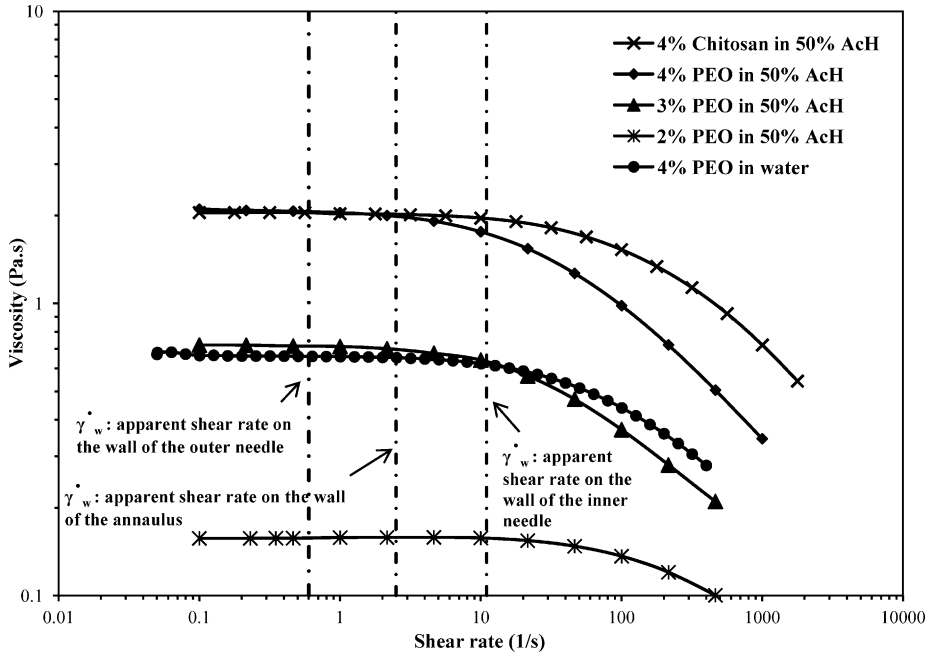

Figure 2. Dependence of viscosity on shear rate for PEO solutions (in water and 50 wt % acetic acid) and chitosan in 50 wt % acetic acid (data collected at 25 °C).

based on preliminary tests. All experiments were carried out at ambient temperature and a relative humidity of 15−20%.

PEO Extraction. The prepared electrospun mats were peeled from the aluminum surface of the collector and submerged in water for 24 h. The extracted mats were then vacuum-dried at 40 °C overnight to remove the absorbed water and further kept in a desiccator at room temperature.

Film Preparation. For comparison and characterization purposes, chitosan/PEO films were prepared by mixing the two master solutions at different ratio (100/0, 50/50, 80/20, and 0/100). Thin films were prepared by pouring and spreading approximately 10 g of the relevant solutions in plastic Petri dishes. The cast films were vacuum-dried at 40 °C overnight to evaporate completely the solvent. The dried films were peeled from the Petri dish and kept in a desiccator at room temperature for subsequent testing.

Characterization. *Rheological Measurements.* Dynamic and steady shear rheological properties of the solutions were characterized at 25 °C, using a stress-controlled rheometer (AR-2000, TA Instruments, DE, U.S.A.) with a Couette flow geometry. Low viscosity silicon oil was used to cover the surface of the sample solutions to prevent evaporation of the solvent during testing. The presence of the oil was shown not to impact the rheological measurements. The stability of the solutions was examined as a function of time in oscillatory shear tests under a low frequency of 1 rad/s and a small deformation of 0.1. Over 1 h, the elastic and loss modulus decreased by less than 1 and 3%, respectively, showing the solutions to be stable. Steady simple shear measurements were carried out by applying shear rates from 0.0625 to 2000 s^{-1}. Possible fluid inertia effects at high shear rates were also examined by looking at values of the Reynolds number Re in Couette flow geometry, this number is given by $Re = \rho\dot{\gamma}h^2/\eta$, where ρ is the density of the fluid, $\dot{\gamma}$ is the shear rate, h is the flow gap, and η is the viscosity of the solution.[35] The calculated Re values were of the order of 10^{-4} to 1 over the range of shear rates used in these tests, hence, the flow conditions were considered inertialess. The zero-shear viscosity of the solutions was estimated by applying the Carreau−Yasuda model[36] to the shear viscosity data.

Surface Morphology and Core−Shell Structure. The surface morphology of the electrospun nanofibers was characterized using a Hitachi S-4700 field emission scanning electron microscope (FE-SEM) operating at 5−10 kV. Samples were cut from co-electrospun mats collected on aluminum foil. These samples were mounted on aluminum stubs and sputter-coated by an ultrathin layer of platinum. The samples were observed at magnifications between 100 and 40000 times of their original size to evaluate their electrospinnability through the presence of beads or droplets. Fiber diameters were also determined using Image-J (National Institutes of Health (NIH), http://rsb.info.nih.gov/ij/) image processing software. For each electrospun mat, at least 150 fibers were considered from three different images to calculate the average diameter.

The core−shell structure of the prepared nanofibers was characterized by transmission electron microscopy (TEM, JEOL, JEM 2100 F). For TEM observation, fibers were directly deposited onto a TEM copper mesh. The copper mesh was then submerged in water, dried and observed again by TEM to discriminate the components in the shell and core regions.

Thermal Analysis. Bulk compositional analysis of the nanofibrous mats was carried out according to the method proposed by Desai et al.[12] using a TA Instruments thermal gravimetric analyzer (TGA, Q 500). Neat PEO, chitosan powder, and electrospun mats were weighted (typical weights of 5−10 mg) and heated from room temperature to 1000 °C under a constant heating rate of 10 °C/min. All the TGA tests were performed under a nitrogen atmosphere. The weight loss for chitosan and PEO in the nanofibers was evaluated by taking the first-order derivative of the raw weight loss thermograms. The area under the respective degradation temperature peak is related to the polymer content in the blends

Fourier Transform Infrared Spectroscopy (FTIR). The local compositional and chemical characteristics of the samples were evaluated by Fourier transform infrared spectroscopy measurements (Perkin-Elmer spectrum 65 FTIR-ATR instrument). Transmission and ATR spectra were recorded at room temperature on the as-cast chitosan and PEO films and as-spun nanofibrous mats, at wavelengths in the range of 700−4000 cm^{-1} (resolution 4 cm^{-1}, accumulation of 128 scans). The chitosan to PEO relative ratio in the samples was estimated from the absorbance ratio at 1550 and 1250 cm^{-1} (A_{1550}/A_{1250}), which are characteristic peaks of chitosan and PEO, respectively.[37]

Crystalline Structure. The crystalline structure of the electrospun nanofibers was investigated using XRD and DSC. Wide angle X-ray diffraction (WAXD) measurements were performed on a diffractometer system (Bruker Discover, D8, 40 kV, 30 mA) equipped with a monochromic Cu Kα (1.542° A) X-ray source, The XRD patterns

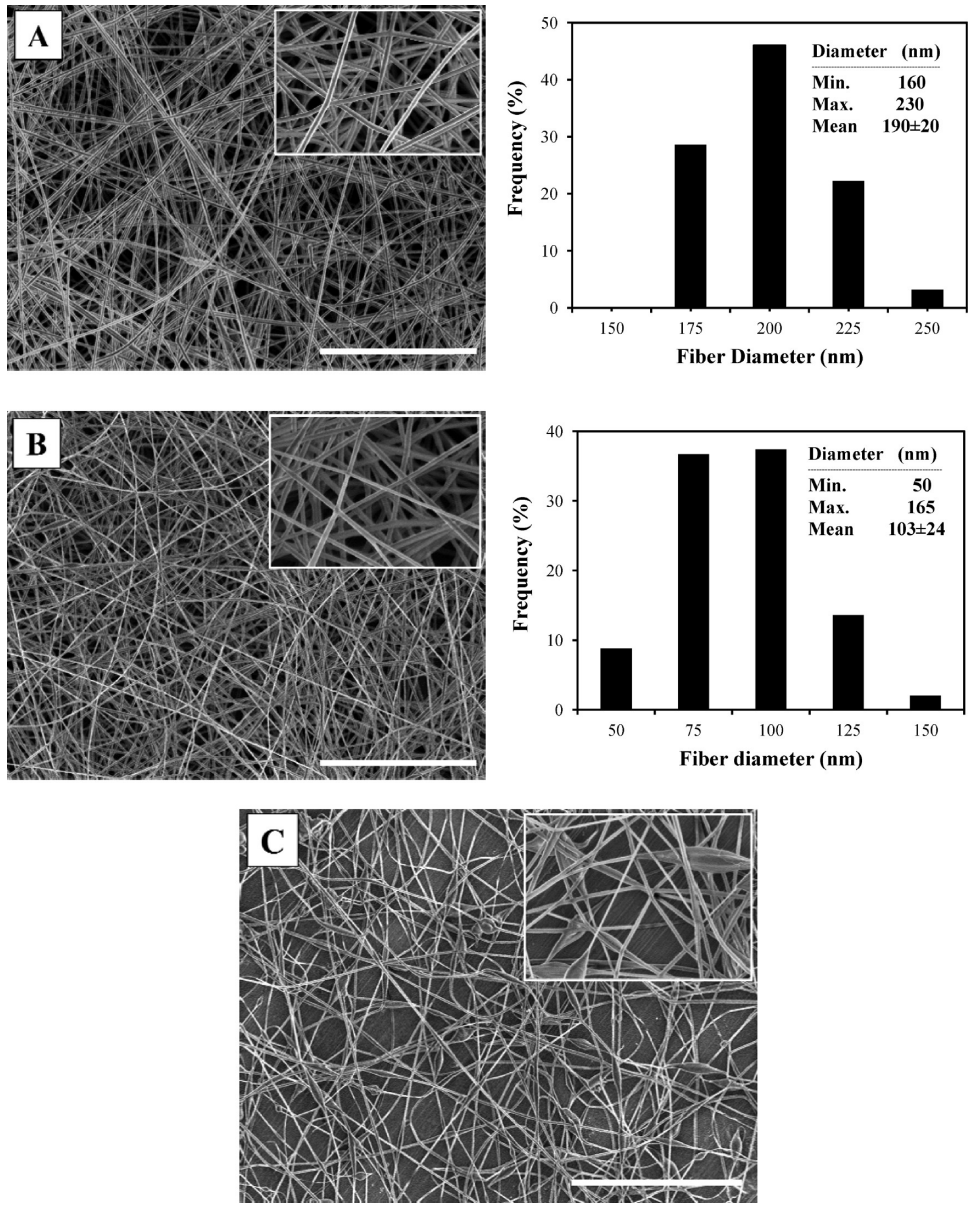

Figure 3. SEM micrograph and diameter histogram of coaxial electrospun nanofibers of PEO/chitosan; scale bars represent 10 μm: (A) 4 wt % PEO, (B) 3 wt % PEO, and (C) 2 wt % PEO (flow rate 0.5 mL/h, needle to collector distance = 15 cm, voltage = 15 kV).

were recorded over a diffraction angle (2θ) range from 5 to 40° in 0.02° steps. Differential scanning calorimetry was carried out using a TA Instrument Q 1000 system. Samples of 6−10 mg were sealed in aluminum pans and heated under a helium atmosphere from 10 to 200 °C in the DSC instrument at a rate of 10 °C/min.

Surface Chemistry (XPS). X-ray photoelectron spectrophotometry (XPS, Thermo Scientific, VG ESCALAB 3 MKII) was used to characterize the surface chemistry of the electrospun mats, in conjunction with a flood gun to eliminate any charging of the surfaces under study. The chemical composition of the sample surface was determined for all elements contained in the polymers except hydrogen, with a typical sampling thickness of 5−10 nm. An Mg Kα monochromatized X-ray source (1253.6 eV) was used to produce photoelectron emission from the samples. The pressure in the analysis chamber was maintained at 10^{-9} Torr. An area of 2 × 3 mm^2 (maximum allowable) was used to scan the surface of the samples to account for surface variations and obtain an averaged signal. Survey spectra were taken to identify the chemical species on the sample surface, and a high resolution scan for C, N, and O was performed to identify the elemental peaks. XPS data was analyzed using VGS 5000 software to calculate the atom percentage of the various elements found on the mat surface. Peak fitting was performed on the high resolution elemental scans (average of 10 scans) to obtain surface chemistry information. Energy calibration was carried out by placing the hydrocarbon peak in the C1s spectrum at 285 eV.

Specific Surface Area (BET) Measurement. The surface area of the electrospun mats was obtained by a Quantachrome instrument BET Autosorb IQ. A gas mixture of nitrogen and helium was continuously fed through the sample cell, which was kept in liquid nitrogen. The total volume of adsorbed nitrogen gas on the surface was measured at different pressures. The volume of gas needed to create an adsorbed monomolecular layer was calculated as follows:[38]

$$\frac{P}{P^0\left[\upsilon\left(1-\left(\frac{P}{P^0}\right)\right)\right]} = \frac{1}{\upsilon_m C} + \frac{C-1}{\upsilon_m C}\frac{P}{P^0} \quad (1)$$

where P is the experimental pressure, P^0 the saturation pressure, υ the volume of the adsorbate, υ_m the volume of gas required to form an

dx.doi.org/10.1021/bm201444v | *Biomacromolecules* 2012, 13, 412−421

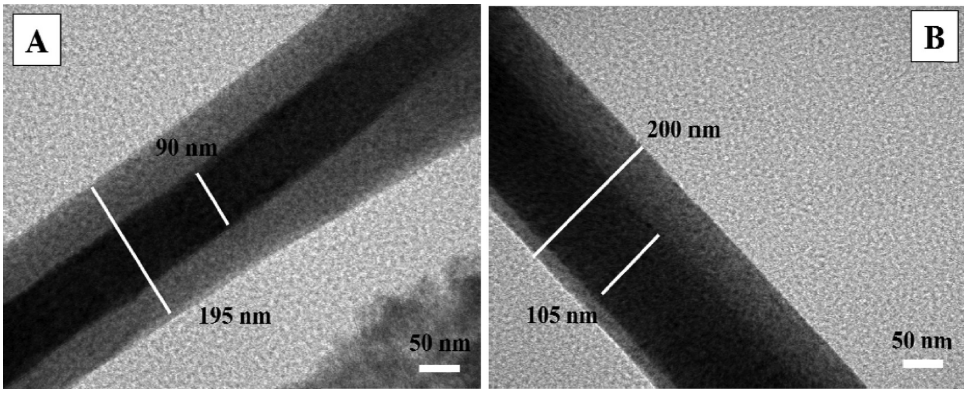

Figure 4. TEM micrographs of core−shell structured PEO-chitosan bicomponent electrospun nanofibers, showing segments of the nanofibers with sharp boundaries; (A) concentric and (B) eccentric core and shell structures (flow rate = 0.5 mL/h, needle to collector distance = 15 cm, voltage = 20 kV).

absorbed monomolecular layer, and C a constant. The procedure for estimating the surface area from eq 1 can be found in ref 39.

RESULTS AND DISCUSSION

Rheological Behavior of Solutions. The rheological characteristics of chitosan and PEO solutions were measured to gain knowledge of their flow behavior in the needles during the electrospinning process (Figure 2). The apparent shear rate at the respective needle walls was approximated by considering the solutions as Newtonian fluids and applying eq 2:

$$\dot{\gamma} = \frac{4Q}{\pi R^3} \tag{2}$$

where $\dot{\gamma}$ is the apparent shear rate at the needle wall, Q is the volumetric flow rate, and R is the radius of the needle (255 μm for the inner needle, 685 μm for the outer needle, and 415 μm at the annulus). For a typical flow rate of 0.5 mL/h, the calculated shear rates are approximately 11, 0.60, and 2.5 s^{-1} at the three respective needle walls, and these values are illustrated in Figure 2 by dotted lines. The viscosity curves in Figure 2 indicate that the solutions are nearly Newtonian at these operating shear rates in the coaxial needle, which support the use of eq 2.

All solutions show a well developed zero-shear viscosity plateau. Shear-thinning is observed at higher shear rates, and this behavior is amplified with polymer content due to more disentanglement between polymer chains. The PEO solution shows more shear-thinning than chitosan at the same polymer content as well as an earlier onset of shear-thinning, indicative of a larger characteristic time. This can be attributed to the different conformations of their chains in the solution state, that is, very flexible for PEO and rigid (rod-like) for chitosan. The zero-shear viscosity of 4 wt % PEO in water is nearly the same as 3 wt % PEO in 50 wt % acid (0.7 Pa·s), however, this value is much less than (almost one-third) that of 4 wt % PEO in 50 wt % acetic acid (2.1 Pa·s). The larger viscosity of PEO in aqueous acetic acid solution, versus water, could be due to interactions between ether groups in PEO and hydroxyl groups in acetic acid that may expand the polymer conformation in solution.[13]

Morphology and Internal Structure of the Coaxial Electrospun Nanofibers. Figure 3 shows the SEM images and associated diameter histograms of the nanofibers produced by the coaxial electrospinning of PEO and chitosan solutions in the core and shell streams, respectively. Defect-free, beadless, and geometrically uniform nanofibers could be prepared when 4 and 3 wt % PEO solutions were fed as the core stream (Figure 3A and B, respectively). However, the morphology was changed to beaded fibers when the concentration of PEO was reduced to 2 wt % (Figure 3C). The same trend was observed for the lower flow rate of 0.25 mL/h. The average diameter of the nanofibers decreased from 190 ± 20 to 103 ± 24 nm (for the flow rate of 0.5 mL/h) by decreasing the PEO concentration from 4 to 3 wt % in the core solution (Figure 3A,B). For the 0.25 mL/h flow rate, the average diameter of the nanofibers were 170 ± 21 and 90 ± 19 nm for 4 and 3 wt % core PEO concentrations, respectively. It shows that the effect of the core solution concentration in the coaxial electrospinning geometry is similar to that for simple electrospinning, that is, an increase in solution concentration generally results in a larger fiber diameter.[40] On the other hand, coaxial electrospinning of a 4 wt % PEO in water as the inner stream and chitosan solution as the outer solution did not result in a stable jet and fiber formation (results not shown). Electrospinnability of neat PEO solutions alone (in 50 wt % aqueous acetic acid) in the same setup has been also studied by removing the outer chitosan stream from the spinneret. It shows that defect-free nanofibers were formed from 3 and 4 wt % PEO concentrations, however, beaded nanofibers and unstable jet were observed for the 2 wt % PEO solution. Moreover, electrospinning of neat chitosan solution alone led to the formation of beads and droplets on the collector. This could be due to too few chain entanglements for successful electrospinning.[24]

It is believed that in this coaxial setup, the PEO solution serves as a spinning aid to successfully prepare nanofibers from the nonelectrospinnable chitosan solution. It is hypothesized that during the coaxial electrospinning process, the core PEO solution carries out the shell chitosan solution through the formation of a stable Taylor cone and continuous jet ejection during the entire process. This could be attributed to a combination of parameters: (a) Using the same solvent in the two streams that leads to low interfacial tension between the two solutions is in favor of successful coaxial electrospinning.[32,41] This is supported by the fact that when the core solvent was changed to water (4 wt % PEO), even though the viscosity is almost the same as the core solution of 3 wt % PEO in 50 wt % acetic acid (Figure 2), no nanofibers were formed. (b) Higher conductivity of the shell solution; chitosan is a polyelectrolyte in solution that makes it more conductive than neutral solution of PEO.[24] Yu et al.[32] speculated that

higher conductivity in the shell layer compared to that of the core stream could stabilize the co-electrospinning process, probably due to the high shear stress applied on the core material and subsequent elongational force, resulting in a thinner core. (c) Low vapor pressure of the solvent (50 wt % acetic acid solution) that was used to make the core and shell solutions (boiling point of acetic acid = 120 °C). It was shown that high vapor pressure solvents may produce unstable Taylor cones in coaxial electrospinning.[41,42] Moreover, as we showed in our previous work[24] specific hydrogen bonds are formed between chitosan and PEO. Those bonds could occur during the coaxial electrospinning process according to Li and Xia[43] results and would stabilize further the jet.

The detailed morphology of the produced coaxial PEO/chitosan nanofibers is shown in a TEM micrograph in Figure 4. The contrast which is created by electron beam diffraction represents the distinctive phases in the nanofibers. These dark and bright regions represent the core and shell of the nanofiber, respectively. The diameters of the shell and core are approximately 200 and 100 nm, respectively. Complete concentricity is observed for the majority of the produced nanofibers (Figure 4A), however, eccentricity are noted for some others (Figure 4B). It is speculated that the nature of the bending instability and whipping motion of the charged jet in the electrospinning process may cause some eccentricity.

To confirm further the formation of the core−shell structure and identify their respective components, the electrospun material deposited on a TEM copper mesh was soaked in water and dried and examined again. The resulting structure shown in Figure 5 reveals that the core region is completely removed and

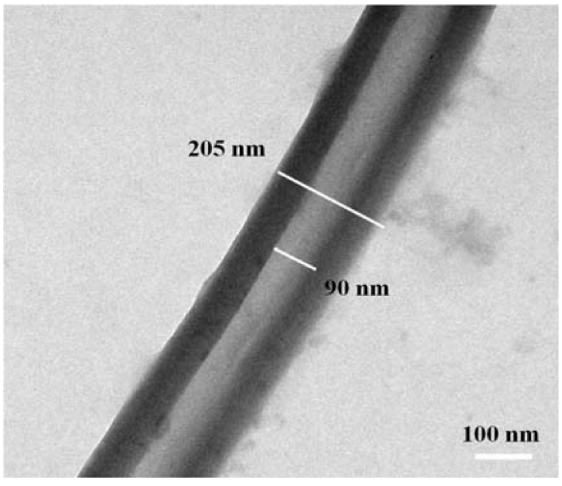

Figure 5. TEM micrograph of a hollow chitosan nanofiber obtained after water extraction of the PEO core (flow rate = 0.5 mL/h, needle to collector distance = 15 cm, voltage = 20 kV).

that a hollow nanofiber is obtained due to the high solubility of PEO in water. Hence, the extraction step reveals that PEO is mainly located in the core while chitosan constitutes the shell of the nanofiber. This is indeed a relatively simple method to produce chitosan hollow nanofibers.

Structural Features of the Core−Shell Nanofibers; Compositional Analysis of Nanofibers. To determine the PEO content, electrospun mat samples were weighed before and after the extraction by water. A weight reduction of 46 ± 4 wt % was measured, in close agreement with the 50/50 PEO/chitosan flow rates used in the process. The resulting mat also kept its mechanical integrity in the form of a membrane after the soaking in water. A typical SEM image of a coaxial electrospun PEO/chitosan nanofibrous mat with PEO extracted is shown in Figure S1 in the Supporting Information. To quantify further the bulk composition of chitosan and PEO in the produced coaxial nanofibers, TGA was used. Raw TGA thermograms and their first-order derivative curves for as-spun and PEO extracted coaxial nanofibrous mats, in comparison with neat chitosan and PEO, are shown in Figure 6. The neat

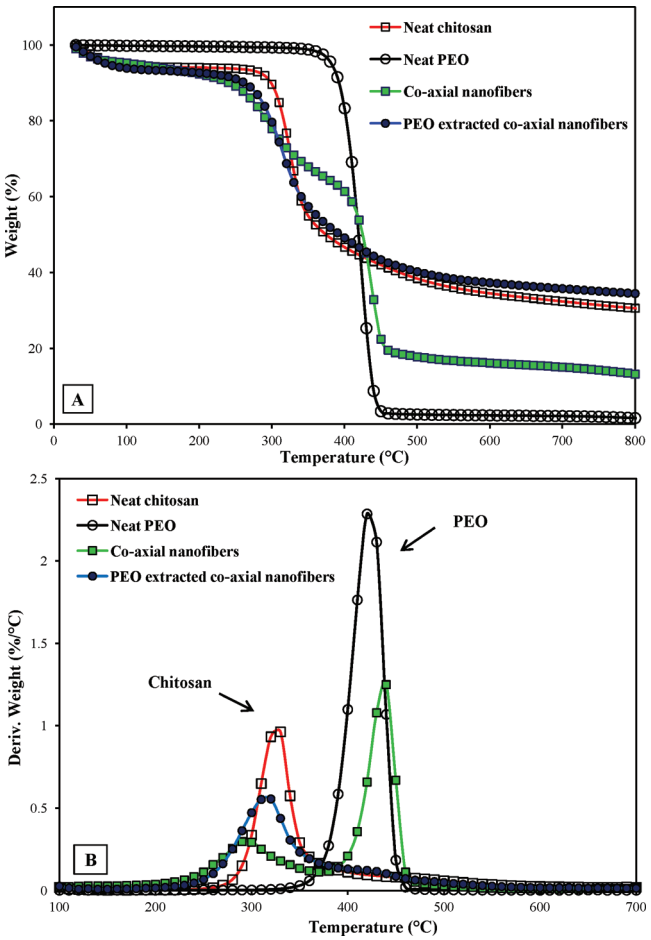

Figure 6. TGA curves of as-spun and PEO extracted coaxial electrospun PEO/chitosan mats compared with neat chitosan and PEO powder: (A) raw TGA curves and (B) first-order derivative of TGA curves.

chitosan sample in Figure 6A shows a weight reduction of 6.5 ± 0.5% until 100 °C due to the evaporation of the adsorbed water. In the case of PEO, at 1000 °C there is nearly no residue left, while an ash residue of 28.11 ± 1.16% is observed in the case of chitosan. The neat PEO and chitosan show two separate decomposition temperatures at 414.5 ± 2 and 325.8 ± 0.73 °C, respectively (Figure 6A). As shown in Figure 6B, the peak temperatures related to PEO and chitosan decomposition were also observed in the coaxial nanofibers, with only a slight shift in their position that has been attributed to the interactions between PEO and chitosan.[24,44] In addition, in the case of the PEO extracted coaxial mat, the PEO peak disappears as expected and only the chitosan peak is observed, with a curve quite similar to that of the neat chitosan (Figure 6B). These

dx.doi.org/10.1021/bm201444v | Biomacromolecules 2012, 13, 412−421

results also reveal that the extraction step is quite efficient in removing PEO from the nanofibers core.

The data obtained from the TGA thermograms is used to determine the content of PEO and chitosan in the produced coaxial nanofibers, considering the humidity and residue level in the mats. This is achieved by measuring the related area under the peaks in the first-order derivative of the TGA curves (Figure 6B). When this method is used, the chitosan content is calculated to be 52 ± 3% for the coaxial electrospun mats, which agrees with the value obtained from the extraction method (~54 wt %).

To evaluate the local compositional homogeneity of the membranes, FTIR analysis has been performed on the samples. Figure 7 shows the ATR-FTIR spectra of as-spun and PEO

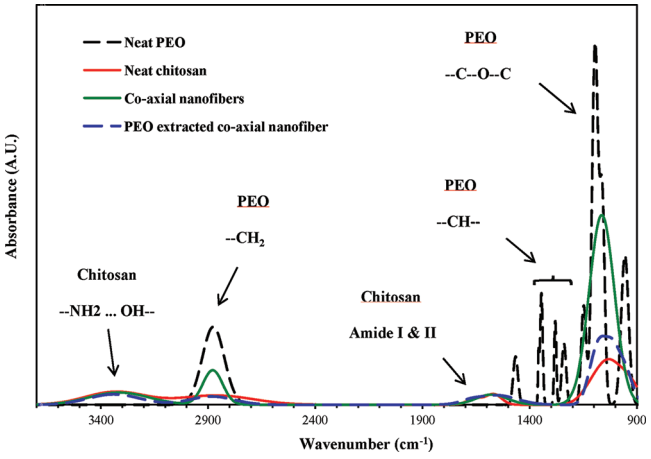

Figure 7. ATR-FTIR spectra of neat chitosan and PEO powder and coaxial electrospun PEO/chitosan nanofibers: as-spun and after extracting PEO by water.

extracted coaxial electrospun nanofibers. Neat chitosan and PEO cast films were also characterized for comparison. Neat chitosan exhibits a broad band around 3100−3500 cm^{-1} and another one at 1550 cm^{-1}, which are commonly attributed to the N−H and O−H stretching of the primary amino groups (due to hydrogen bonds with O−H groups) and N−H stretching of the secondary amides (known as Amide II), respectively.[14,45,46] Very weak peaks for the stretching of the carbonyl (C═O-NHR) groups at 1650 cm^{-1} (known as Amide I) and C−H stretching at 2880 cm^{-1} also appear. The neat PEO shows its FTIR absorption feature bands around 2880, which are assigned to the CH_2 stretching; however, this band overlaps with that detected for chitosan. Other feature bands of PEO are observed at 1150, 1110, and 1060 cm^{-1} as triplet peaks related to C−O−C stretching vibrations, and sharp peaks at 1360, 1340, 1275, and 1250 cm^{-1} attributed to CH deformation of the methyl groups.[13,46] The absorbance intensity ratio at 1550 and 1250 cm^{-1} (A_{1550}/A_{1250}) is used as an indication of the chitosan to PEO ratio.[37] Therefore, local compositions of chitosan and PEO are determined by evaluating this ratio in different areas of the coaxial nanofibers by recording the transmission FTIR spectra for that region. It is found that the A_{1550}/A_{1250} ratio does not vary significantly for various locations of the samples, confirming the uniformity and homogeneity of the prepared nanofibers and the stability of the electrospinning process. A chitosan content of 55 ± 1.6% was calculated based on this ratio and is, again, in close agreement with the values obtained from bulk compositional analysis, that is, the extraction test (~54%) and TGA (52 ± 1.6%).

In addition, after washing the coaxial electrospun mat with water, the feature peaks of PEO disappear and the spectra obtained is that of neat chitosan (Figure 7). Therefore it can be concluded that after PEO washing, a nanofibrous mat exclusively made of chitosan can be obtained.

Crystalline Structure of the Nanofibers. To evaluate the crystalline structure, DSC and XRD tests have been performed on chitosan/PEO electrospun nanofibers and compared with results for neat chitosan and PEO. DSC thermograms of as-spun and washed coaxial electrospun nanofibers, and nanofibers prepared from a 50/50 chitosan/PEO blend solution are presented in Figure 8. DSC curves of neat chitosan and PEO

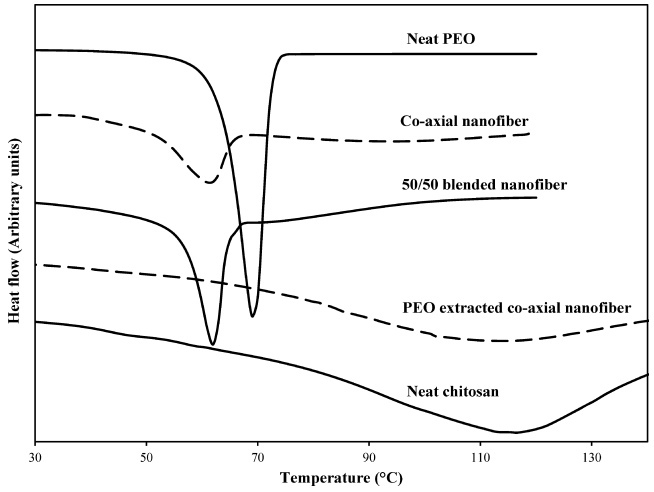

Figure 8. DSC thermograms of neat chitosan and PEO powder, as-spun and washed coaxial electrospun PEO/chitosan nanofibers, and 50/50 blend chitosan/PEO nanofibers.

powder are also shown for comparison purposes. The broad endothermic peak in the chitosan curve is attributed to the evaporation of bound water from chitosan.[13] For the neat PEO powder, a sharp endothermic melting peak around 71 °C is observed. On the other hand, the coaxial PEO-chitosan nanofibers show a melting transition at 62.1 °C. This peak disappears after PEO extraction and the DSC curve become similar to that of the neat chitosan powder (Figure 8). The nanofibers from the 50/50 chitosan/PEO blend solution also exhibit an endothermic melting transition, closely located to that of the coaxial nanofibers. Table 1 shows melting point and

Table 1. Melting Point and Enthalpy of Fusion of Neat PEO Powder and Electrospun Nanofibers

sample	T_m (°C)	ΔH (J/g; PEO)
PEO powder	69.0 ± 1.0	180.8
PEO nanofiber	64.5 ± 1.7	165.5
coaxial nanofibers	62.1 ± 2.0	158.7
50/50 blend nanofibers	62.0 ± 1.6	157.1

enthalpy of fusion for neat PEO powder and nanofiber in comparison with coaxial electrospun nanofibers and 50/50 blended chitosan/PEO nanofibers. It shows that the melting point and enthalpy of fusion (hence, crystallinity) in the PEO nanofibers decrease as compared to that of the neat powder. This is attributed to the very fast evaporation of the solvent in

the electrospinning process that may prevent the crystals to form completely.[47,48] In the case of nanofibers based on blend (50/50), interactions between chitosan and PEO chains in the nanofibers may also hinder the crystallization of PEO.[46]

To further illustrate the differences in crystalline content and morphology of the nanofibers and neat materials, X-ray diffraction patterns were obtained. Figure 9 presents the XRD

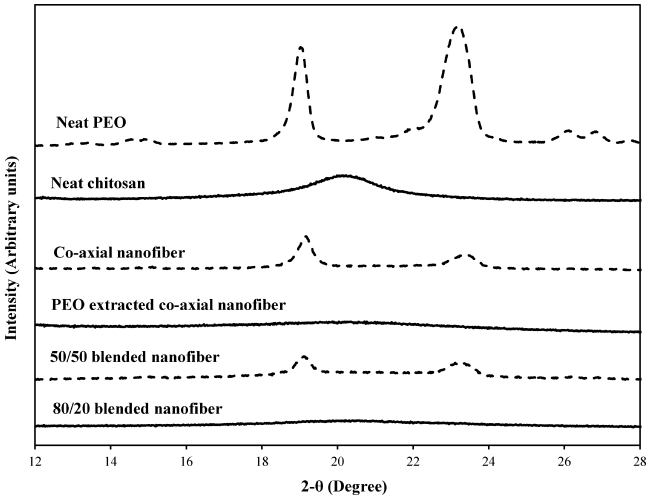

Figure 9. XRD diffraction pattern of neat chitosan and PEO powder, coaxial electrospun PEO-chitosan nanofibers: as-spun and after extracting the PEO by water and blended chitosan/PEO nanofibers (80/20 and 50/50 chitosan/PEO blend ratios).

patterns of neat chitosan and PEO powder, coaxial PEO-chitosan nanofibers before and after washing, and 50/50 and 80/20 blend chitosan/PEO nanofibers. The neat PEO powder show two sharp feature peaks around 2θ = 19.1° and 2θ = 23.2°.[47] The peak appearing around 2θ = 20.1° is characteristic of chitosan and has a much lower intensity than those of PEO, indicating that the crystalline ordering in chitosan is significantly less than in PEO.[11] The two peaks related to the PEO crystals also appear in the XRD patterns of the coaxial nanofibers and the 50/50 blended chitosan/PEO nanofibers; however, the peak around 2θ = 23.2° is weaker than for the neat PEO powder. Nevertheless, it depicts the existence of the same PEO crystalline structure in the electrospun nanofibers, with a crystallinity degree slightly lower than in the neat material, as indicated previously by the DSC results. The difference between the intensity of the main peaks in the neat PEO powder as compared to its electrospun counterparts may be related to the orientation of the PEO crystals according to the strong elongational field in the electrospinning process, and possibly also to less crystals formed.[49] No peak is observed after PEO washing from the coaxial mats, which reveals once more the complete removal of PEO and a remaining chitosan amorphous structure. This indicates that the crystalline microstructure of chitosan cannot build up as well as PEO in the electrospinning process, most probably due to the fast evaporation of the solvent in this process. Additionally, in the case of the 80/20 blend chitosan/PEO nanofibers, the low amount of PEO and the presence of chitosan−PEO interactions hinder crystal formation and lead to an almost amorphous structure.

Surface Properties of Core−Shell Nanofibers. X-ray photo electron spectroscopy (XPS) analysis was performed to quantify the surface composition of the coaxial electrospun nanofibers. The XPS survey spectra (data not shown here) and the surface elemental content of carbon, oxygen, and nitrogen of the coaxial and blended chitosan/PEO electrospun nanofibers, as well as cast films of the neat components, were analyzed by the XPS technique. Chitosan contains nitrogen in its amine and acetylamine groups on its backbone; however, PEO has only oxygen and carbon in its structure. Figure 10

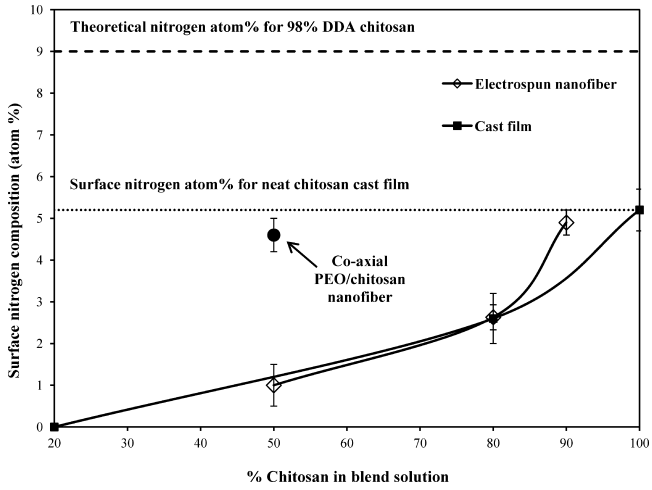

Figure 10. Surface nitrogen composition of the blended chitosan/PEO electrospun nanofibers and their cast films. The point represents the coaxial PEO/chitosan electrospun mats.

shows the surface nitrogen composition in electrospun nanofibers and cast films vs chitosan content in the blend (or feed) solutions. The theoretical nitrogen composition for a 97.5% DDA chitosan, calculated from the chemical structure and ratios of the repeating units in chitosan,[2] is calculated to be 9% and is shown as the dashed line in Figure 10. It can be observed from Figure 10 that this value is not in close agreement with the surface nitrogen composition of neat chitosan film measured by XPS, that is, 5.2% (shown as dotted line in Figure 10). This discrepancy between the theoretical nitrogen composition and the surface nitrogen composition measured by XPS has been previously reported[2,50] for surface analysis of chitosan containing films. This can be attributed to a contaminating overlayer on the surface or the film surface composition is not necessarily the same as its expected theoretical stoichiometric bulk composition. As expected, the surface nitrogen composition increases with chitosan content, and for the 90/10 chitosan/PEO blend the nitrogen composition is close to that of neat chitosan (cast film). In the 50/50 chitosan/PEO blend, the surface nitrogen content is very low (∼ 1%); however, in coaxial electrospun nanofibers, this value increases to 4.6 ± 0.6%, a value very close to that of the neat chitosan cast film. This is another indication of the successful formation of a core/shell nanostructure, with a chitosan shell.

The actual specific surface area of the electrospun coaxial nanofibers, neat chitosan powder, and chitosan cast film were obtained through conventional N_2 adsorption measurements based on the Brunauer−Emmett−Teller (BET) theory.[38] A specific surface area of 15 ± 1.5 m^2/g was calculated for the coaxial nanofibers prepared from a 0.5 mL/h flow rate, a value that is much higher than that of chitosan powder (less than 1 m^2/g) and most probably film. The specific surface area of the

nanofibers was also calculated theoretically by considering the fibers as cylinders and neglecting the area of the cross sections, based on eq 3:

$$A = \frac{4000}{D \times \rho} \quad (3)$$

where A is the specific surface area in g/m^2 and D and ρ denote the diameter (in nm) and density (in g/cm^3) of the nanofibers, respectively. The theoretical surface area of the coaxial nanofibers was calculated to be 16.7 m^2/g, considering 190 nm as the average diameter and 1.26 g/cm^3 for the density of the nanofibers (detailed on page 3 of the Supporting Information). This value is in good agreement with the experimental result (15 ± 1.5 m^2/g).

CONCLUSIONS

Chitosan is a cationic biopolymer that is challenging to electrospin. In this work we were able to produce fairly uniform sized core/shell structured PEO/chitosan nanofibers using a coaxial electrospinning technique. PEO and chitosan solutions were fed as core and sheath materials to a cospinneret, respectively. Core−shell structure of the nanofibers was observed by TEM images. Presence of chitosan on the shell was confirmed by TEM images of hollow nanofibers obtained after extracting the PEO content. The obtained mats after the washing step were comprised of nearly 100% chitosan in the form of hollow nanofibers. The presence of chitosan on the surface was also confirmed by XPS analysis as further evidence of core/shell formation. Bulk and local compositional analysis of chitosan and PEO in the electrospun nanofibers showed that the ratio of chitosan to PEO in the nanofibers was similar to that in the feed streams and also that the local composition of the prepared nanofibers was homogeneous, indicating the stability of the electrospinning process. Due to a shell layer entirely made of chitosan, this processing method has several advantages such as the simplicity of a one-step production without any post-treatment, with the possibility of producing chitosan hollow nanofibers through a subsequent PEO water washing. These nanofibers have interesting potential applications in the biomedical field such as purification of the blood in hemodialysis and wound dressings.

ASSOCIATED CONTENT

Supporting Information

SEM micrograph of a PEO extracted nanofibrous mat; density calculation of the coaxial nanofibers. This material is available free of charge via the Internet at http://pubs.acs.org.

AUTHOR INFORMATION

Corresponding Author

*Phone: 01-514 340 4711, ext. 5390 (M.-C.H.); 01-514 340 4711, ext. 3703 (A.A.). E-mail: marie-claude.heuzey@polymtl.ca (M.-C.H.); abdellah.ajji@polymtl.ca (A.A.).

ACKNOWLEDGMENTS

The authors gratefully acknowledge the financial support of NSERC (National Science and Engineering Research Council of Canada) and FRQNT (Fonds de recherche du Québec - Nature et technologies). We are also thankful to Mesdames Weawkamol Leelapornpisit and Suzie Poulin for their great help in the morphological and XPS studies. Messrs. Daniel Dumas and Robert Delisle are appreciated for the design and fabrication of the nanofibers collecting system, and the authors express great gratitude to Mrs. Melina Hamdine for her coordination in assembling the electrospinning set up.

REFERENCES

(1) An, J.; Zhang, H.; Zhang, J. T.; Zhao, Y. H.; Yuan, X. Y. *Colloid Polym. Sci.* **2009**, *287*, 1425−1434.
(2) Desai, K.; Kit, K.; Li, J. J.; Davidson, P. M.; Zivanovic, S.; Meyer, H. *Polymer* **2009**, *50*, 3661−3669.
(3) Haider, S.; Park, S. Y. *J. Membr. Sci.* **2009**, *328*, 90−96.
(4) Ye, P.; Xu, Z. K.; Wu, J.; Innocent, C.; Seta, P. *Biomaterials* **2006**, *27*, 4169−4176.
(5) Ignatova, M. G.; Manolova, N. E.; Toshkova, R. A.; Rashkov, I. B.; Gardeva, E. G.; Yossifova, L. S.; Alexandrov, M. T. *Biomacromolecules* **2010**, *11*, 1633−1645.
(6) Wang, W.; Itoh, S.; Konno, K.; Kikkawa, T.; Ichinose, S.; Sakai, K.; Ohkuma, T.; Watabe, K. *J. Biomed. Mater. Res., Part A* **2009**, *91A*, 994−1005.
(7) Cooper, A.; Bhattarai, N.; Zhang, M. Q. *Carbohydr. Polym.* **2011**, *85*, 149−156.
(8) Zhou, Y. S.; Yang, D. Z.; Chen, X. M.; Xu, Q.; Lu, F. M.; Nie, J. *Biomacromolecules* **2008**, *9*, 349−354.
(9) Li, D.; Xia, Y. N. *Adv. Mater.* **2004**, *16*, 1151−1170.
(10) Greiner, A.; Wendorff, J. H. *Angew. Chem., Int. Ed.* **2007**, *46*, 5670−5703.
(11) Rinaudo, M. *Prog. Polym. Sci.* **2006**, *31*, 603−632.
(12) Desai, K.; Kit, K.; Li, J.; Zivanovic, S. *Biomacromolecules* **2008**, *9*, 1000−1006.
(13) Duan, B.; Dong, C. H.; Yuan, X. Y.; Yao, K. D. *J. Biomater. Sci., Polym. Ed.* **2004**, *15*, 797−811.
(14) Li, L.; Hsieh, Y. L. *Carbohydr. Res.* **2006**, *341*, 374−381.
(15) McKee, M. G.; Wilkes, G. L.; Colby, R. H.; Long, T. E. *Macromolecules* **2004**, *37*, 1760−1767.
(16) McKee, M. G.; Hunley, M. T.; Layman, J. M.; Long, T. E. *Macromolecules* **2006**, *39*, 575−583.
(17) Ohkawa, K.; Minato, K. I.; Kumagai, G.; Hayashi, S.; Yamamoto, H. *Biomacromolecules* **2006**, *7*, 3291−3294.
(18) Schiffman, J. D.; Schauer, C. L. *Biomacromolecules* **2007**, *8*, 594−601.
(19) Geng, X. Y.; Kwon, O. H.; Jang, J. H. *Biomaterials* **2005**, *26*, 5427−5432.
(20) Homayoni, H.; Ravandi, S. A. H.; Valizadeh, M. *Carbohydr. Polym.* **2009**, *77*, 656−661.
(21) Sangsanoh, P.; Supaphol, P. *Biomacromolecules* **2006**, *7*, 2710−2714.
(22) Klossner, R. R.; Queen, H. A.; Coughlin, A. J.; Krause, W. E. *Biomacromolecules* **2008**, *9*, 2947−2953.
(23) Bhattarai, N.; Edmondson, D.; Veiseh, O.; Matsen, F. A.; Zhang, M. Q. *Biomaterials* **2005**, *26*, 6176−6184.
(24) Pakravan, M.; Heuzey, M. C.; Ajji, A. *Polymer* **2011**, *52*, 4813−4824.
(25) Ignatova, M.; Manolova, N.; Markova, N.; Rashkov, I. *Macromol. Biosci.* **2009**, *9*, 102−111.
(26) Zhang, H. T.; Wu, C. Y.; Zhang, Y. L.; White, C. J. B.; Xue, Y.; Nie, H. L.; Zhu, L. M. *J. Mater. Sci.* **2010**, *45*, 2296−2304.
(27) Shalumon, K. T.; Anulekha, K. H.; Girish, C. M.; Prasanth, R.; Nair, S. V.; Jayakumar, R. *Carbohydr. Polym.* **2010**, *80*, 413−419.
(28) Park, W. H.; Jeong, L.; Yoo, D. I.; Hudson, S. *Polymer* **2004**, *45*, 7151−7157.
(29) Torres-Giner, S.; Ocio, M. J.; Lagaron, J. M. *Carbohydr. Polym.* **2009**, *77*, 261−266.
(30) Chen, Z. G.; Mo, X. M.; Qing, F. L. *Mater. Lett.* **2007**, *61*, 3490−3494.
(31) Sun, Z. C.; Zussman, E.; Yarin, A. L.; Wendorff, J. H.; Greiner, A. *Adv. Mater.* **2003**, *15*, 1929−1932.
(32) Yu, J. H.; Fridrikh, S. V.; Rutledge, G. C. *Adv. Mater.* **2004**, *16*, 1562−1566.

(33) Ojha, S. S.; Stevens, D. R.; Hoffman, T. J.; Stano, K.; Klossner, R.; Scott, M. C.; Krause, W.; Clarke, L. I.; Gorga, R. E. *Biomacromolecules* **2008**, *9*, 2523−2529.
(34) Modrzejewska, Z.; Eckstein, W. *Biopolymers* **2004**, *73*, 61−68.
(35) Yosick, J. A.; Giacomin, J. A.; Stewart, W. E.; Ding, F. *Rheol. Acta* **1998**, *37*, 365−373.
(36) Carreau, P. J.; De Kee, D.; Chabra, P. R. *Rheology of Polymeric Systems: Principles and Applications*; Hanser Publishers: Munich, 1997.
(37) Kriegel, C.; Kit, K. M.; McClements, D. J.; Weiss, J. *Polymer* **2009**, *50*, 189−200.
(38) Brunauer, S.; Emmett, P. H.; Teller, E. *J. Am. Chem. Soc.* **1938**, *60*, 309−319.
(39) Li, J.; Favis, B. D. *Polymer* **2001**, *42*, 5047−5053.
(40) Fridrikh, S. V.; Yu, J. H.; Brenner, M. P.; Rutledge, G. C. *Phys. Rev. Lett.* **2003**, *90* (144502), 1−4.
(41) Li, D.; Babel, A.; Jenekhe, S. A.; Xia, Y. N. *Adv. Mater.* **2004**, *16*, 2062−2066.
(42) Moghe, A. K.; Gupta, B. S. *Polym. Rev.* **2008**, *48*, 353−377.
(43) Li, D.; Xia, Y. N. *Nano Lett.* **2004**, *4*, 933−938.
(44) Lewandowska, K. *Thermochim. Acta* **2009**, *493*, 42−48.
(45) Jia, Y. T.; Gong, J.; Gu, X. H.; Kim, H. Y.; Dong, J.; Shen, X. Y. *Carbohydr. Polym.* **2007**, *67*, 403−409.
(46) Zivanovic, S.; Li, J. J.; Davidson, P. M.; Kit, K. *Biomacromolecules* **2007**, *8*, 1505−1510.
(47) Deitzel, J. M.; Kleinmeyer, J.; Harris, D.; Tan, N. C. B. *Polymer* **2001**, *42*, 261−272.
(48) Son, W. K.; Youk, J. H.; Lee, T. S.; Park, W. H. *Polymer* **2004**, *45*, 2959−2966.
(49) Zhang, J. F.; Yang, D. Z.; Xu, F.; Zhang, Z. P.; Yin, R. X.; Nie, J. *Macromolecules* **2009**, *42*, 5278−5284.
(50) Matienzo, L. J.; Winnacker, S. K. *Macromol. Mater. Eng.* **2002**, *287*, 871−880.